Journal of Hydraulic Research Vol. 47, No. 1 (2009), pp. 41–49
doi:10.3826/jhr.2009.2865

Application of the method of characteristics to the dam break wave problem

Application de la méthode des caractéristiques au problème de l'onde de rupture de barrage

HUBERT CHANSON, (IAHR Member), Professor in Civil Engineering, *The University of Queensland, Brisbane QLD 4072, Australia. Fax: (61 7) 3365 4599, E-mail: h.chanson@uq.edu.au, Url: http://www.uq.edu.au/~e2hchans/*

ABSTRACT
In dam break waves, the surge front is a sudden discontinuity characterized by extremely rapid variations of flow depth and velocity. In this study, simple analytical solutions for instantaneous dam break wave are developed using the method of characteristics. The solutions are obtained for initially dry horizontal and sloping channels with turbulent motion, and they are compared with several data sets obtained in large-size facilities. A main feature of the development is its simplicity that is well-suited to students and young professionals.

RÉSUMÉ
Dans les ondes de rupture de barrage, le front d'onde est une discontinuité soudaine caractérisée par des variations extrêmement rapides de tirant d'eau et de vitesse. Dans cette étude, des solutions analytiques simples sont développées pour l'onde d'une rupture de barrage instantanée en utilisant la méthode des caractéristiques. Les solutions sont obtenues pour des canaux horizontaux et en pente initialement à sec, avec un écoulement turbulent; elles sont comparées à plusieurs ensembles de mesures obtenues dans les équipements de grande taille. Une caractéristique principale de ce développement est sa simplicité qui est bien adaptée aux étudiants et aux jeunes professionnels.

Keywords: Analytical solutions, bed friction effect, dam break wave, method of characteristics

1 Introduction

Dam break waves have been responsible for numerous losses of life (e.g. Fig. 1). Related situations include flash flood runoff in ephemeral streams, debris flow surges and tsunami runup on dry coastal plains. In all cases, the surge front is a sudden discontinuity characterized by extremely rapid variations of flow depth and velocity. Dam failures motivated basic studies on the dam break wave, including the milestone contribution by Ritter (1892) following the South Fork (Johnstown) dam disaster (USA, 1889). Physical modeling of dam break wave is relatively limited despite a few basic experiments (Table 1). In retrospect, the experiments of Schoklitsch (1917) were well ahead of their time, and demonstrated that Armin von Schoklitsch (1888–1968) had a solid understanding of both physical modeling and dam break processes. Well-known analytical studies of the dam break on dry channel include Dressler (1952) and Whitham (1955) for a horizontal channel, while Hunt (1982, 1984) solved the surge flow down a sloping channel. Note that all analytical solutions assumed an instantaneous dam break.

Today, dam break wave predictions are often based upon numerical predictions, validated by limited data sets. For the period 2003–2004, the international database The Web of Science™ listed 40 journal articles on dam break including 34 numerical studies, 4 experimental studies and only one theoretical development. Albeit research initiatives, there has been a lack of basic theoretical analyzes for the past 30 years. Current knowledge of dam break wave in dry channels remains rudimentary despite a few studies (e.g. Dressler, 1954; Escande *et al.*, 1961; Lauber, 1997; Chanson, 2004b). There are also contradictory arguments on the flow fundamentals. For example, some measurements highlighted a boundary layer region in the surging wave leading edge (e.g. Mano, 1984; Davies, 1988; Fujima and Shuto, 1990; Chanson, 2004b), while others indicated quasi-ideal fluid vertical velocity distributions (Estrade, 1967; Wang, 2002; Jensen *et al.*, 2003).

This study describes simple analytical solutions for instantaneous dam break wave based upon the method of characteristics. The solutions are developed for initially dry horizontal and sloping channels with turbulent motion, and the results are compared with several data sets obtained in large-size facilities. It is the aim of this work to provide simple explicit solutions of dam break wave problems that are easily understood by students, young researchers, and professionals.

Revision received March 19, 2007/Open for discussion until August 31, 2009.

Figure 1 Photograph of the St Francis dam, USA (March 12, 1928) (Courtesy of Santa Clarita Valley Historical Society)—Looking upstream with onlookers in the foreground, in front of a 65 m high dam wall section

2 Basic equations and solution for a dry horizontal channel

A dam break wave is the flow resulting from a sudden release of a mass of fluid in a channel. For 1D applications, the continuity and momentum equations yield the Saint-Venant equations. For a prismatic rectangular channel, the dimensionless equations are

$$\frac{\partial d}{\partial t} + d\frac{\partial V}{\partial x} + V\frac{\partial d}{\partial x} = 0 \quad (1)$$

$$\frac{\partial V}{\partial t} + V\frac{\partial V}{\partial x} + \frac{\partial d}{\partial x} + (S_f - S_o) = 0, \quad (2)$$

where d is the dimensionless depth ($d = d'/d'_o$), V is the dimensionless flow velocity, t is the dimensionless time, x is the dimensionless co-ordinate ($x = x'/d'_o$), S_o is the bed slope ($S_o = \sin\theta$), θ is the angle between the bed and the horizontal with $\theta > 0$ for a downward slope, and S_f is the friction slope. The dash ($'$) is used to denote dimensional variables: e.g., d'_o

Table 1 Characteristics of turbulent dam break wave experiments in dry rectangular channels

Reference (1)	Bed slope θ (2)	Channel characteristics (3)	Reservoir characteristics (4)	Remarks (5)
Schoklitsch (1917)	0	(1) $L' = 26$ m, $B' = 0.6$ m (2) $L' = 150$ m, $B' = 1.3$ m	(1) d'_o up to 0.25 m (2) d'_o up to 1 m	
Dressler (1954)	0	$L' = 65$ m, $B' = 0.225$ m (a) Painted timber; (b) Coarse sand paper; (c) Strips (slats): $h' = 0.00635$ m, $l' = 0.0254$ m	$d'_o = 0.055$, 0.11 and 0.22 m	
Fauré and Nahas (1961)	0.0069°	$L' = 40.6$ m, $B' = 0.25$ m 2 types of roughness	$d'_o = 0.23$ m	$S_o = 1.2\,\mathrm{E}-4$
Cavaillé (1965)	0	$L' = 40$ m, $B' = 0.25$ m Glass walls and steel invert. (a) Smooth invert. (b) Rough invert (cylindrical elements $\varnothing' = 20$ mm in zigzag, $l' = 28$ mm, $h' = 8$ mm)	$L'_{res} = 18$ m, rectangular reservoir (a) $d'_o = 0.115$, 0.23 m (b) $d'_o = 0.23$ m	
Estrade (1967)	0	(1) $L' = 23.65$ m, $B' = 0.50$ m (a) Smooth invert; (b) Rough invert (rough cement)	(1) $d'_o = 0.20$ & 0.40 m, $L'_{res} = 13.65$ m, rectangular reservoir	
		(2) $L' = 23.65$ m, $B' = 0.25$ m (a) Smooth invert; (b) Rough invert (cylindrical elements $\varnothing' = 20$ mm in zigzag, $l' = 28$ mm, $h'' = 6$ mm)	(2) $d'_o = 0.30$ m, $L'_{res} = 0.70$ m, rectangular reservoir	
Lauber (1997)	0	$L' = 2$ m, $B' = 0.5$ m PVC invert	$0.15 \leq d'_o \leq 0.6$ m, $L'_{res} < 3.6$ m, rectangular reservoir	
	5.7°, 26.5°	$L' = 14$ m, $B' = 0.5$ m PVC invert	$d'_o = 0.3$ m, $L'_{res} < 3.6$ m, trapezoidal reservoir	Vertical gate
Chanson *et al.* (2000)	0	$L' = 15$ m, $B' = 0.8$ m Smooth paint invert	Reservoir volume: 0.9 to 1 m^3, $q(t=0)' = 0.15$ to 0.17 m^2/s	Free-jet discharging vertically at one end of channel

Notes: B': channel width; d'_o: reservoir height; h': (strip/element) roughness height; L': total channel length; L'_{res}: upstream reservoir length; l': longitudinal spacing between (strip) roughness element. All experiments were conducted with tap water.

is the initial reservoir height. The Saint-Venant equations cannot be solved analytically usually because of nonlinear terms: e.g., the friction slope $S_f = f/2V'^2/(gD'_H)$, where D'_H is the hydraulic diameter and f is the Darcy-Weisbach friction factor. A mathematical technique to solve the system of partial differential equations formed by the Saint-Venant equations is the method of characteristics which yields a characteristic system of equations

$$\frac{d}{dt}(V + 2C) = (S_o - S_f) \quad \text{along} \quad \frac{dx}{dt} = V + C \tag{3a}$$

$$\frac{d}{dt}(V - 2C) = (S_o - S_f) \quad \text{along} \quad \frac{dx}{dt} = V - C \tag{3b}$$

where C is the dimensionless celerity of a small disturbance. For a rectangular channel $C = 1$.

For a frictionless dam break in a wide horizontal channel, the analytical solution of Eqs (1) and (2) yields Ritter's solution (Ritter, 1892)

$$U = 2, \tag{4}$$

where U is the dimensionless wave front celerity. At a given time, the dimensionless free-surface and velocity profile between the leading edge of the negative wave and the wave front are

$$\frac{x}{t} = 2 - 3\sqrt{d} \qquad \text{for } -1 \le \frac{x}{t} \le +2 \tag{5}$$

$$V = \frac{2}{3}\left(1 + \frac{x}{t}\right) \quad \text{for } -1 \le \frac{x}{t} \le +2 \tag{6}$$

where t is the dimensionless time from dam break. Equations (5) and (6) were first derived by Barré de Saint-Venant (1871) for a frictionless positive surge in a horizontal channel.

2.1 *Turbulent dam break wave: a simple solution*

The turbulent dam break flow is analyzed as an ideal-fluid flow region behind a flow resistance-dominated tip zone (Fig. 2). Whitham (1955) introduced this conceptual approach, but his mathematical development differs from the present simple solution.

In the ideal fluid flow region, the characteristic system of equations become

$$\frac{d}{dt}(V + 2C) = 0 \quad \text{along} \quad \frac{dx}{dt} = V + C \tag{7}$$

$$\frac{d}{dt}(V - 2C) = 0 \quad \text{along} \quad \frac{dx}{dt} = V - C \tag{8}$$

In the wave tip region ($x_1 \le x \le x_s$, Fig. 2), the flow velocity does not vary rapidly in the forward tip zone and experimental data showed that it is about the wave front celerity U (Dressler, 1954; Estrade, 1967; Lauber, 1997; Liem and Köngeter, 1999). If the flow resistance is dominant, and the acceleration and inertial terms are small, the dynamic wave equation (Eq. (2)) may reduce to a diffusive wave equation. For a horizontal channel, it yields

$$\frac{\partial d}{\partial x} + \frac{f}{8}\frac{U^2}{d} = 0 \quad \text{Wave tip region} \tag{9}$$

The integration of Eq. (9) gives the shape of the wave front

$$d = \sqrt{\frac{f}{4}U^2(x_s - x)} \tag{10}$$

assuming a constant Darcy–Weisbach friction factor for $x_1 \le x \le x_s$, where x_s is the dimensionless wave front location ($x_s = x'_s/d'_o$) (Chanson, 2005). Next to the leading edge of the wave, the slope of the free-surface becomes important to counterbalance the flow resistance.

At the transition between ideal fluid and wave tip regions ($x = x_1$), the flow depth and velocity must be continuous.

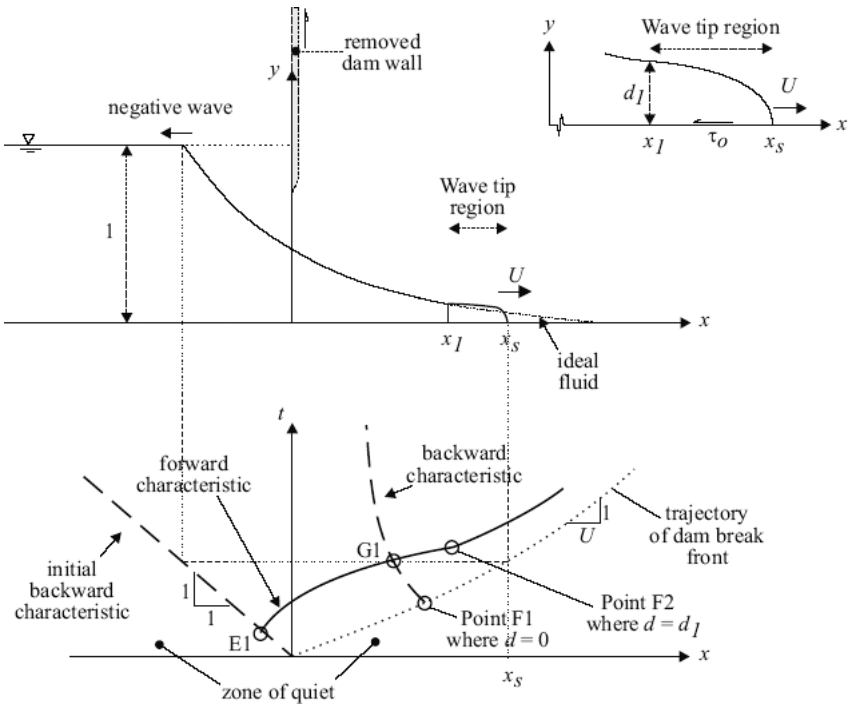

Figure 2 Sketch of the dam break wave in a dry horizontal channel

The flow properties (d_1, V_1) must satisfy

$$d_1 = \frac{1}{9}\left(2 - \frac{x_1}{t}\right)^2 = \sqrt{\frac{f}{4}U^2(x_s - x_1)} \tag{11a}$$

$$V_1 = U = \frac{2}{3}\left(1 + \frac{x_1}{t}\right). \tag{11b}$$

The conservation of mass must be satisfied. The mass of fluid in the wave tip region ($x_1 \leq x \leq x_s$) must equal the mass of fluid in the ideal fluid flow profile for $x_1 \leq x \leq 2t$

$$\int_{x_1}^{x_s} \sqrt{\frac{f}{4}U^2(x_s - x)}dx = \int_{x_1}^{2t} \frac{1}{9}\left(2 - \frac{x}{t}\right)^2 dx. \tag{12}$$

The conservation of mass (Eq. (12)) may be integrated analytically. After substitution and re-arrangement, it yields an exact solution in terms of the wave front celerity

$$\frac{8}{3}\frac{1}{f}\frac{\left(1 - \frac{U}{2}\right)^3}{U^2} = t. \tag{13}$$

The wave front location equals

$$x_s = \left(\frac{3}{2}U - 1\right)t + \frac{4}{fU^2}\left(1 - \frac{U}{2}\right)^4 \tag{14}$$

and the free-surface profile satisfies

$$d = \frac{1}{9}\left(2 - \frac{x}{t}\right)^2 \quad -t \leq x \leq \left(\frac{3}{2}U - 1\right)t \tag{15a}$$

$$d = \sqrt{\frac{f}{4}U^2(x_s - x)} \quad \left(\frac{3}{2}U - 1\right)t \leq x \leq x_s \tag{15b}$$

The location of the transition between ideal and friction dominated flow regions is given by Eq. (11b). Equation (13) gives a direct relationship between the dimensionless wave front celerity U and dimensionless time t. Equation (14) yields the dimensionless wave front location as a function of the dimensionless wave front celerity. Equations (15) and (11b) give the entire dimensionless free-surface profile $d = F(x/t)$. The results yield an explicit expression of the wave front celerity, wave front location, and free-surface and velocity profiles (Chanson, 2005).

3 Dam break wave in a horizontal channel

The assumption of constant friction factor f in the wave tip region is a gross approximation since the flow depth is zero and the shear stress is infinite at the wave front leading edge. For turbulent motion, the flow resistance may be approximated by the Altsul formula

$$f = 0.1\left(1.46\frac{k_s'}{D_H'} + \frac{100}{\text{Re}}\right)^{1/4}, \tag{16}$$

where k_s' is the equivalent sand roughness height, D_H' is the hydraulic diameter, and Re is the flow Reynolds number (Idelchik, 1969, 1994; Chanson, 2004a). The Altsul formula is a slightly less-accurate formula that may be used to initialize the calculation with the Colebrook–White formula. Assuming that Eq. (16) holds in unsteady flows, and for a wide channel (i.e. $D_H' \approx 4d'$), it may be rewritten in the wave tip region as

$$f = \frac{1}{d^{1/4}}\left(3.65 \times 10^{-5}k_s + \frac{2.5 \times 10^{-3}}{\text{Re}_d U}\right)^{1/4}, \tag{17}$$

where $\text{Re}_d = \rho\sqrt{gd_o^3}/\mu$ is analogous to a Reynolds number and k_s is a dimensionless equivalent roughness height ($k_s = k_s'/_o'$). Re_d is called the dam reservoir flow Reynolds number. It is a function of fluid properties and initial flow conditions only.

The integration of the diffusive wave equation (Eq. (8)) yields the shape of wave tip region

$$d = \left(\frac{9}{32}\left(3.65 \times 10^{-5}k_s + \frac{2.5 \times 10^{-3}}{\text{Re}_d U}\right)^{1/4} U^2(x_s - x)\right)^{4/9}. \tag{18}$$

The flow properties must be continuous at the transition between the ideal-fluid region and the wave tip zone. The continuity equations must be further satisfied and its integration yields an analytical solution in terms of the dimensionless wave front celerity

$$\frac{32}{13}\frac{\left(1 - \frac{U}{2}\right)^{7/2}}{U^2\left(3.65 \times 10^{-5}k_s + \frac{2.5\times10^{-3}}{\text{Re}_d U}\right)^{1/4}} = t. \tag{19}$$

The wave front location equals

$$x_s = \left(\frac{3}{2}U - 1\right)t + \frac{32}{9}\frac{\left(1 - \frac{U}{2}\right)^{9/2}}{U^2\left(3.65 \times 10^{-5}k_s + \frac{2.5\times10^{-3}}{\text{Re}_d U}\right)^{1/4}} \tag{20}$$

and the free-surface profile satisfies

$$d = \frac{1}{9}\left(2 - \frac{x}{t}\right)^2 \quad -t \leq x \leq \left(\frac{3}{2}U - 1\right)t \tag{21a}$$

$$d = \left(\frac{9}{32}\left(3.65 \times 10^{-5}k_s + \frac{2.5 \times 10^{-3}}{\text{Re}_d U}\right)^{1/4} U^2(x_s - x)\right)^{4/9} \quad \left(\frac{3}{2}U - 1\right)t \leq x \leq x_s \tag{21b}$$

Analytical results are shown in Figs 3–6 for several flow conditions where they are compared with relevant experimental data. In the particular cases of smooth-turbulent and fully rough turbulent flows, the above results may be simplified (e.g. Chanson, 2005).

3.1 Discussion: comparison with experimental data

The analytical solutions were compared with well-known analytical solutions (Dressler, 1952; Whitham, 1955) and with experimental data obtained in large-size facilities (Table 1). Comparisons were performed in terms of wave front location, wave front celerity and instantaneous free-surface profiles. Some examples are presented in Figs 3–6 while details of experimental investigations are summarized in Table 1. Overall the comparative analyses showed a good agreement between the present

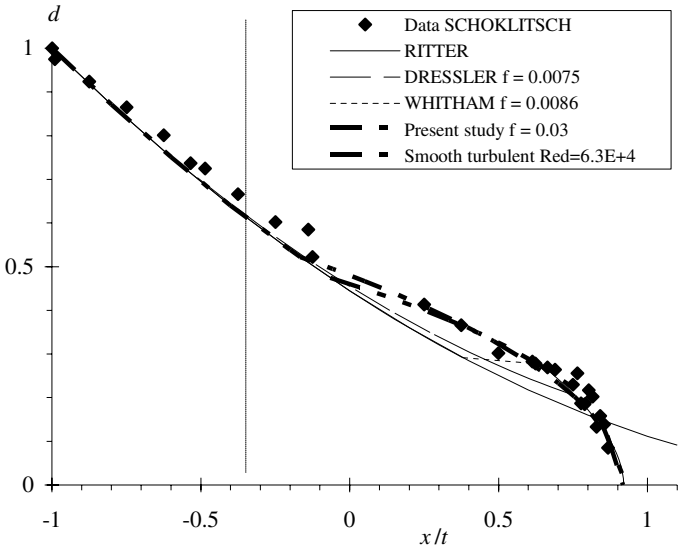

Figure 3 Dimensionless instantaneous free-surface profiles—Comparison between Eq. (15) assuming $f = 0.03$, Eq. (20) and Dressler's (1952) theory, Whitham's (1955) theory and experimental data (Schoklitsch, 1917; $d'_o = 0.074$ m, $t' = 9.4$ s)

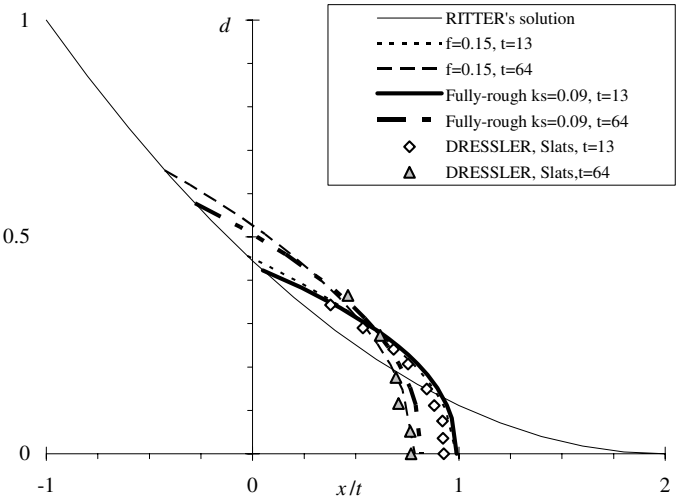

Figure 4 Dimensionless instantaneous free-surface profiles—Comparison between Eq. (15) assuming $f = 0.15$, Eq. (21) ($k_s = 0.09$), and experimental data (Dressler, 1954; $d'_o = 0.22$ m, slat invert (strip))

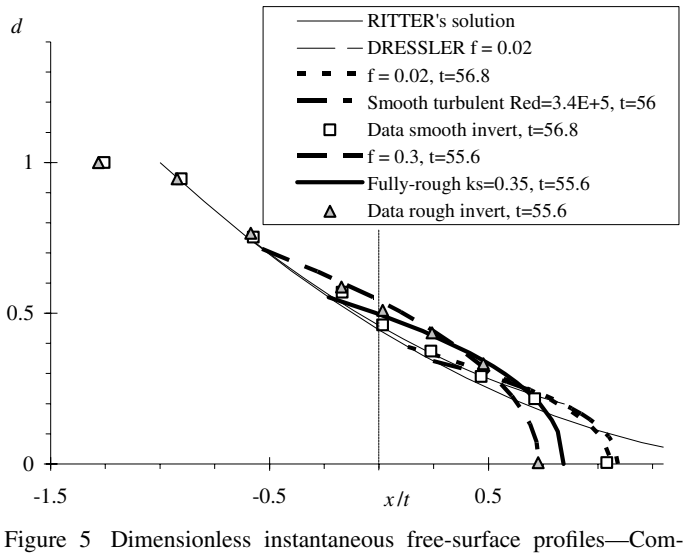

Figure 5 Dimensionless instantaneous free-surface profiles—Comparison between smooth-invert and rough-invert dam break wave for $t = 56$ – Smooth-invert: Cavaillé's (1965) data ($d'_o = 0.23$ m, smooth invert), Dressler's (1952) theory ($f = 0.02$), Eq. (15) assuming $f = 0.02$, and Eq. (21); Rough-invert: Cavaillé's (1965) data ($d'_o = 0.23$ m, rough invert), Eq. (14) assuming $f = 0.3$, and Eq. (21) ($k_s = 0.35$)

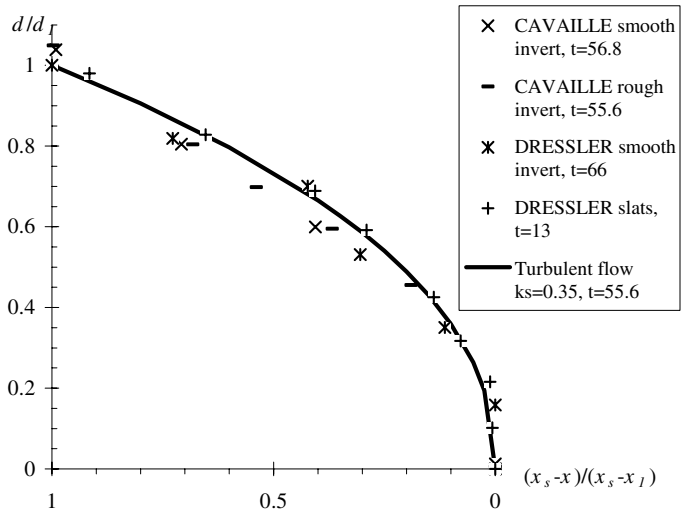

Figure 6 Dimensionless free-surface profile d/d_1 in the wave tip region—Comparison between Eq. (18) and the data of Dressler (1954) and Cavaillé (1965)

analysis and more advanced solutions as well as experimental data. For example, Fig. 3 presents a comparison between a data set by Schoklitsch (1917), Ritter's (1892) solution, analytical solutions by Dressler's (1952) and Whitham's (1955), Eqs (15) and (21). Figure 4 shows a data set obtained on rough invert (Dressler, 1954; slat invert) that is compared with Eqs (12) and (21). Figure 5 illustrates more specifically the effect of bed roughness on dam break wave. Two data sets are shown at a same dimensionless time ($t = 56$) for smooth- and rough inverts. Data and calculations indicate a slower wave front celerity on rough invert, associated with a thicker wave front region.

The agreement between analytical solutions and experimental data is dependent upon the flow resistance estimate, namely the selection of the relative roughness k_s (Eq. (21)) or upon the selection of friction factor f (Eq. (15)). Accurate calibrations must be performed using instantaneous free-surface profiles. These provide a Lagrangian description on the flow. Alternate techniques based upon wave front location and celerity, or fixed point measurements, are less accurate. In the present study, for the data sets listed in Table 1, the relative roughness k_s (Eq. (21)), or the friction factor f (Eq. (15)), were found to be independent of time and experimental flow conditions for a given type of invert roughness. The results were further consistent between independent data sets (Chanson, 2005).

Figure 6 presents the shape of the wave front, with the dimensionless water depth d/d_1 as a function of the dimensionless

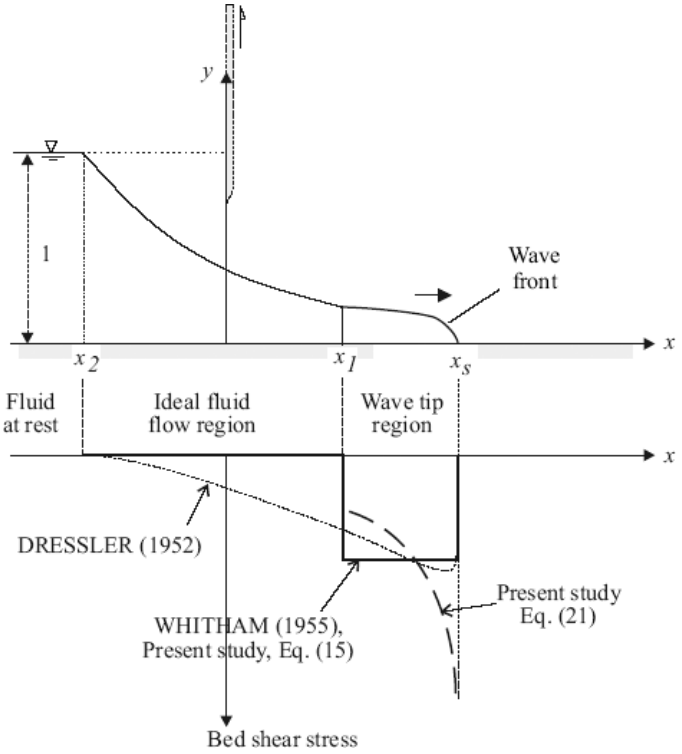

Figure 7 Sketch of longitudinal distributions of bed shear stress in turbulent dam break wave—Comparison between the theoretical models of Dressler (1952), Whitham (1955), and present study (Eqs (15) and (21))

distance $(x_s - x)/(x_s - x_1)$, where the subscripts s and 1 refer, respectively, to the wave leading edge and to the transition between ideal fluid and wave tip regions. Note the close agreement between Eq. (18), and the experimental data.

In this study, Eqs (15) and (21) are based upon two different longitudinal distributions of boundary shear stress. This is illustrated in Figure 7 showing the differences in longitudinal bed shear stress distributions between the different theoretical models. Yet all theories gave close results in terms of wave front celerity and instantaneous free-surface profiles and good agreement with experimental data. All these suggest little effects of some discontinuity at $x = x_1$. In fact the approximation of a constant Darcy friction factor f (Dressler, 1952; Whitham, 1955; Present study (Eq. (15)) appears reasonable in comparison with the more sophisticated model (Eq. (21)), although the physics is questionable. This "apparent contradiction" may reflect upon our ignorance of some fundamental turbulent process in the wave front.

4 Dam break wave in a sloping channel with some initial motion

The above approach may be extended to a sloping channel when the flow velocity behind the dam is initially V_o for $t < 0$. Prior to dam break, the translation of both dam and reservoir is frictionless. The sudden dam removal takes place at $t = 0$ when the dam wall is located at $x = 0$. After dam break, the flow is assumed to be an ideal fluid flow region behind a friction dominated wave tip

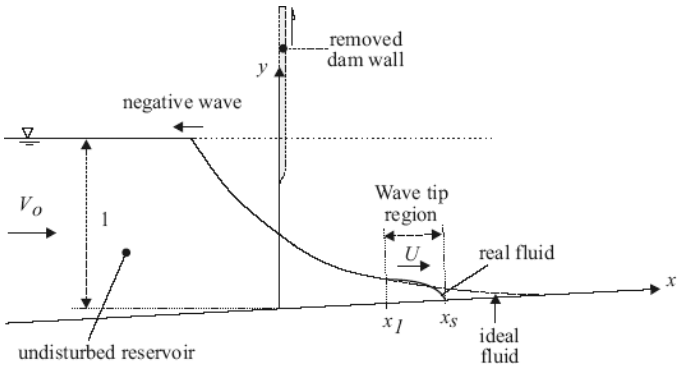

Figure 8 Sketch of a dam break wave in an upward slope with initial flow motion

region, while it is assumed that the translation of the undisturbed reservoir remains frictionless for $t > 0$ (Fig. 8).

In the ideal fluid flow region, Ritter's solution may be extended (Peregrine and Williams, 2001; Chanson, 2005). For a mild slope, the dimensionless flow properties are

$$d = \frac{1}{9}\left(2 + V_o + \frac{1}{2}S_o t - \frac{x}{t}\right)^2 \quad \text{for } V_o - 1 \leq \frac{x}{t} \leq \frac{x_1}{t} \tag{22a}$$

$$C = \frac{1}{3}\left(2 + V_o + \frac{1}{2}S_o t - \frac{x}{t}\right) \quad \text{for } V_o - 1 \leq \frac{x}{t} \leq \frac{x_1}{t} \tag{22b}$$

$$V = \frac{2}{3}\left(1 + \frac{1}{2}V_o + S_o t + \frac{x}{t}\right), \quad \text{for } V_o - 1 \leq \frac{x}{t} \leq \frac{x_1}{t} \tag{22c}$$

where the bed S_o is positive for a downward slope.

In the wave tip region, the flow properties may be deduced using the diffusion wave equation taking into account flow resistance and bed slope

$$\frac{\partial d}{\partial x} + \frac{f}{8}\frac{U^2}{d} - S_o = 0. \quad \text{Wave tip region} \tag{23}$$

The complete integration yields a complicated result that is presented in the Appendix A. A Taylor series expansion of the solution gives the earlier result

$$d = \left(\frac{9}{32}\left(3.65 \times 10^{-5} k_s + \frac{2.5 \times 10^{-3}}{\mathrm{Re}_d U}\right)^{1/4} U^2 (x_s - x)\right)^{4/9} \tag{18}$$

that will be used in first approximation.

The free-surface profile and velocity must be continuous at the transition between the ideal fluid region and the friction-dominated wave tip. The conservation of mass must be also satisfied. The exact solution of the dam break wave in terms of the wave front celerity is

$$\frac{32}{13}\frac{\left(1 + \frac{1}{2}V_o + \frac{1}{2}S_o t - \frac{U}{2}\right)^{7/2}}{U^2\left(3.65 \times 10^{-5} k_s + \frac{2.5 \times 10^{-3}}{\mathrm{Re}_d U}\right)^{1/4}} = t = t, \tag{24}$$

while the wave front location equals

$$x_s = \left(\frac{3}{2}U - \frac{1}{2}V_o - S_o t - 1\right) t + \frac{32}{9}\frac{\left(1 + \frac{1}{2}V_o + \frac{1}{2}S_o t - \frac{U}{2}\right)^{9/2}}{U^2\left(3.65 \times 10^{-5}k_s + \frac{2.5\times 10^{-3}}{\mathrm{Re}_d U}\right)^{1/4}}. \quad (25)$$

The free-surface profile is given by

$$d = \frac{1}{9}\left(2 + V_o + \frac{1}{2}S_o t - \frac{x}{t}\right)^2 \quad \text{for } V_o - 1 \le \frac{x}{t} \le \frac{x_1}{t} \quad (26a)$$

$$d = \left(\frac{9}{32}\left(3.65 \times 10^{-5}k_s + \frac{2.5 \times 10^{-3}}{\mathrm{Re}_d U}\right)^{1/4} U^2(x_s - x)\right)^{4/9} \quad \text{for } \frac{x_1}{t} \le \frac{x}{t} \le \frac{x_s}{t}. \quad (26b)$$

The location of the transition between ideal fluid and wave tip regions is

$$x_1 = \left(\frac{3}{2}U - \frac{1}{2}V_o - S_o t - 1\right) t, \quad (27)$$

Equation (24) provides an explicit relationship between the dimensionless wave front celerity and dimensionless time. Note that the solution in terms of the wave front celerity is nonlinear with the dimensionless time present on both sides of Eq. (24). Equation (25) yields the dimensionless wave front location as a function of the dimensionless wave front celerity and dimensionless time. Equations (26) and (27) give the entire dimensionless free-surface profile.

5 Summary and concluding remarks

New analytical solutions of turbulent dam break wave in dry channels are presented. The flow is analyzed using the conceptual model of Whitham (1955) with a friction-dominated front region followed by an ideal-fluid flow. For a horizontal channel and a semi-infinite reservoir, a series of solutions are derived for turbulent flow assuming a nonconstant Darcy friction factor in the wave front region. The analytical results were validated successfully with experimental data in large-size facilities (Table 1) and by comparison with more-advanced theoretical models. Flow resistance estimates are critical, and instantaneous free-surface profiles are deemed the best validity tests.

A main feature of the developments is the simplicity. The theoretical results yield simple explicit analytical expressions in terms of wave front celerity, wave front location and free-surface profile. They illustrate a simple pedagogical application of the Saint-Venant equations and method of characteristics, linking together the ideal-fluid flow equations yielding Ritter's solution in a horizontal channel, with a diffusive wave equation for the wave tip region. The new solutions (e.g. Eqs (15), (21) and (26)) yield realistic solutions of the dam break wave with bed friction. Both ideal-fluid flow calculations and diffusive wave equations constitute relatively simple lecture materials. At the University of Queensland, the lecture material is taught in an advanced elective to civil and environmental engineering students in fourth year (subject CIVL4120 Advanced open channel flow and design). The explicit analytical solutions provide further validation tools for the numerical integration of the method of characteristics applied to dam break wave. A comparison between numerical results, analytical solutions and experimental results under controlled flow conditions may assist in the accurate selection of flow resistance coefficient and numerical schemes. Finally, the simplicity of the equations may allow some extension to more complicated flow situations and non-Newtonian fluids, for example, like Chanson *et al.* (2006) who applied successfully the mathematical treatment of Hunt (1982) to dam break wave of thixotropic fluids.

Present theoretical solutions are based upon a few key assumptions. These include the assumption $V(x, t) = U(t)$ in the wave tip region, and some discontinuity of $\partial d/\partial x$, $\partial V/\partial x$ and τ_0 at the transition between wave tip and ideal-fluid flow regions (i.e. $x = x_1$). A number of experiments tend to support the first approximation: e.g., Estrade (1967), Liem and Köngeter (1999). These data suggested little longitudinal variations in velocity in the wave tip region. Further comparisons between present solutions and experimental results were successful for a fairly wide range of experimental conditions obtained independently and including instantaneous free-surface profiles, wave front celerity, and wave front locations. These comparisons constitute a solid validation of the proposed theory. It is acknowledged that the present solutions are limited to semi-infinite reservoir, rectangular channel and quasi-instantaneous dam break. The latter approximation is often reasonable for concrete dam failure (e.g. Fig. 1) but it is not applicable to many other applications including embankment breach.

Acknowledgments

The writer acknowledges some helpful exchange with Dr A. Hogg and Professor H. Peregrine (University of Bristol).

Appendix A—Wave front shape in an inclined channel

Considering an instantaneous dam break wave on a mild-sloping invert, the diffusive wave equation in the wave front is

$$\frac{\partial d}{\partial x} + \frac{f}{8}\frac{U^2}{d} - S_o = 0. \quad (A1)$$

For a turbulent flow, the Darcy–Weisbach friction factor f may be approximated by the Altsul formula. For a wide channel, the formula may be written as

$$f = \frac{1}{d^{1/4}}\left(3.65 \times 10^{-5}k_s + \frac{2.5 \times 10^{-3}}{\mathrm{Re}_d U}\right)^{1/4}, \quad (A2)$$

where k_s is the a relative roughness height and $\mathrm{Re}_d = \rho\sqrt{g d_o^3}/\mu$.

Equation (A1) may be rewritten as

$$\frac{\partial d}{\partial t} + \frac{X}{d^{5/4}} = S_o, \tag{A3}$$

where

$$X = \frac{0.1}{8}\left(\frac{1.46}{4}k_s + \frac{100}{4}\frac{1}{U\mathrm{Re}_d}\right)^{1/4} U^2. \tag{A4}$$

The boundary conditions of Eq. (A3) are: $d = 0$ at the wave front ($x = x_s$), and $\partial d/\partial x < 0$ in the wave front. Equation (A3) may be solved analytically. For $S_o \neq 0$, the exact solution is

$$\begin{aligned} S_o(x_s - x) &= 0.020034\left(\frac{X}{S_o}\right)^{4/5} - d - \frac{4}{5}\left(\frac{X}{S_o}\right)^{4/5} \\ &\times \mathrm{Ln}\left(\left(\frac{X}{S_o}\right)^{1/5} - d^{1/4}\right) - \frac{2\sqrt{2(5+\sqrt{5})}}{5}\left(\frac{X}{S_o}\right)^{4/5} \\ &\times \mathrm{ArcTan}\left(-\frac{(-1+\sqrt{5})\left(\frac{X}{S_o}\right)^{1/5} + 4d^{1/4}}{\sqrt{2(5+\sqrt{5})}\left(\frac{X}{S_o}\right)^{1/5}}\right) \\ &- \frac{2\sqrt{10-2\sqrt{5}}}{5}\left(\frac{X}{S_o}\right)^{4/5} \\ &\times \mathrm{ArcTan}\left(\frac{(1+\sqrt{5})\left(\frac{X}{S_o}\right)^{1/5} + 4d^{1/4}}{\sqrt{10-2\sqrt{5}}\left(\frac{X}{S_o}\right)^{1/5}}\right) \\ &- \left(\frac{1}{\sqrt{5}} - \frac{1}{5}\right)\left(\frac{X}{S_o}\right)^{4/5} \mathrm{Ln}\left(\left(\frac{X}{S_o}\right)^{2/5} \right. \\ &\left. - \frac{-1+\sqrt{5}}{2}\left(\frac{X}{S_o}\right)^{1/5} d^{1/4} + \sqrt{d}\right) \\ &+ \left(\frac{1}{\sqrt{5}} + \frac{1}{5}\right)\left(\frac{X}{S_o}\right)^{4/5} \mathrm{Ln}\left(\left(\frac{X}{S_o}\right)^{2/5} \right. \\ &\left. + \frac{1+\sqrt{5}}{2}\left(\frac{X}{S_o}\right)^{1/5} d^{1/4} + \sqrt{d}\right). \end{aligned} \tag{A5}$$

Notation

C = Dimensionless celerity of a small disturbance for an observer travelling with the flow: $C = C'/\sqrt{gd'_o}$
C' = Celerity (m/s) of a small disturbance for an observer travelling with the flow; for a rectangular channel: $C' = \sqrt{gd'_o}$
D'_H = Hydraulic diameter (m)
d = Dimensionless flow depth measured normal to the invert: $d = d'/d'_o$
d' = Flow depth (m) measured normal to the invert
d'_o = Initial reservoir height (m) measured normal to the chute invert
d_1 = Flow depth at the upstream end of the wave tip region: $d_1 = d'_1/d'_o$
f = Darcy–Weisbach friction factor
g = Gravity constant: $g = 9.8$ m/s^2
h' = Roughness element height (m)
k_s = Dimensionless roughness height: $k_s = k'_s/d'_o$
k'_s = Equivalent sand roughness height (m)
L' = Channel length (m)
L'_{res} = Reservoir length (m)
l' = Longitudinal spacing (m) between roughness elements
q' = Volume flow rate per unit width (m^2/s)
Re_d = Dimensionless Reynolds number: $\mathrm{Re}_d = \rho\sqrt{gd_o'^3}/\mu$
S_f = Friction slope: $S_f = f/2V'^2/(gD'_H)$
S_o = Bed slope: $S_o = \sin\theta$
t = Dimensionless time from dam removal: $t = t'\sqrt{g/d'_o}$
t' = Time (s) from dam removal
U = Dimensionless wave front celerity: $U = U'/\sqrt{gd'_o}$
U' = Wave front celerity (m/s)
V = Dimensionless flow velocity: $zV = V'/\sqrt{gd'_o}$
V' = Flow velocity (m/s)
V_o = Initial dimensionless reservoir velocity positive downstream
V_1 = Dimensionless flow velocity at the upstream end of the wave tip region
W' = Channel width (m)
X = Dimensionless parameter: $X = \frac{0.1}{8}\left(\frac{1.46}{4}k_s + \frac{100}{4}\frac{1}{U\mathrm{Re}_d}\right)^{1/4} U^2$
x = Dimensionless longitudinal distance measured from the dam wall: $x = x'/d'_o$
x' = Longitudinal distance (m) measured from the dam wall
x_s = Dimensionless wave front position
x_1 = Dimensionless location at the upstream end of the wave tip region

Greek symbols

μ = Dynamic viscosity (Pa.s)
ν = Kinematic viscosity (m^2/s): $\nu = \mu/\rho$
θ = Bed slope angle
ρ = Fluid density (kg/m^3)
τ'_o = Boundary shear stress (Pa)

Subscript

1 = Flow conditions at the transition between ideal-fluid and wave tip regions
o = Initial flow conditions in the reservoir

Superscript

$'$ = Dimensional variable

References

Barré de Saint-Venant, A.J.C. (1871). Théorie du mouvement non permanent des eaux, avec application aux crues des rivières et à l'introduction des marées dans leur lit. *Comptes Rendus des séances de l'Académie des Sciences*, Paris, France, Séance 17 July 1871, 73, 147–154 (in French).

Cavaillé, Y. (1965). Contribution à l'étude de l'écoulement variable accompagnant la vidange brusque d'une retenue. *Publ. Scient. et Techn. du Ministère de l'Air*, 410, Paris, France, 165 (in French).

Chanson, H. (2004a). The hydraulics of open channel flow: An introduction. *Butterworth-Heinemann*, Oxford, UK, 2nd edn, 630.

Chanson, H. (2004b). Dam break wave propagation on abrupt drops: an experimental study. In: Behnia, M., Lin, W. and McBain, G.D. (eds.), *Proc. 15th Australasian Fluid Mech. Conf., AFMC, Sydney, Australia*, Paper AFMC00014, 4 (CD-ROM).

Chanson, H. (2005). Applications of the Saint-Venant equations and method of characteristics to the dam break wave problem. Report No. CH55/05, Dept. of Civil Engineering, The University of Queensland, Brisbane, Australia, May, 135.

Chanson, H., Aoki, S., Maruyama, M. (2000). Experimental investigations of wave runup downstream of nappe impact. Applications to flood wave resulting from dam overtopping and tsunami wave runup. Coastal/Ocean Engineering Report No. COE00-2, Dept. of Architecture and Civil Eng., Toyohashi University of Technology, Japan, 38.

Chanson, H., Jarny, S., Coussot, P. (2006). Dam break wave of thixotropic fluid. *J. Hydr. Engng. ASCE*, 132(3), 280–293.

Davies, T.R.H. (1988). Debris flow surges—A laboratory investigation. *Mitteilungen der Versuchsanstalt fur Wasserbau, Hydrologie und Glaziologie*, No. 96, ETH-Zurich, Switzerland, 122.

Dressler, R.F. (1952). Hydraulic resistance effect upon the dam-break functions. *J. Res. Natl. Bureau of Standards*, 49(3), 217–225.

Dressler, R. (1954). Comparison of theories and experiments for the hydraulic dam-break wave. *Proc. Int. Assoc. Scientific Hydrology Assemblée Générale*, Rome, Italy, 3 (38), 319–328.

Escande, L., Nougaro, J., Castex, L., Barthet, H. (1961). Influence de quelques paramètres sur une onde de crue subite à l'aval d'un barrage. *J. La Houille Blanche* 5, 565–575 (in French).

Estrade, J. (1967). Contribution à l'étude de la suppression d'un barrage. Phase initiale de l'écoulement. *Bulletin de la Direction des Etudes et Recherches, Series A, Nucléaire, Hydraulique et Thermique*, EDF Chatou, France, No. 1, 3–128 (in French).

Fauré, J., Nahas, N. (1961). Etude numérique et expérimentale d'intumescences à forte courbure du front. *J. La Houille Blanche*, 5, 576–586. Discussion: 5, 587 (in French).

Fujima, K., Shuto, N. (1990). Formulation of frictions laws for long waves on a smooth dry bBed. *Coastal Engng. Japan*, 33(1), 25–47.

Hunt, B. (1982). Asymptotic solution for dam-break problems. *J. Hydr. Div., Proceedings, ASCE*, 108(HY1), 115–126.

Hunt, B. (1984). Perturbation dolution for dam break floods. *J. Hydr. Engng., ASCE* 110(8), 1058–1071.

Idel'cik, I.E. (1969). Mémento des pertes de charge. *Eyrolles Editor*, Collection de la direction des études et recherches d'Electricité de France, Paris, France (in French).

Idelchik, I.E. (1994). *Handbook of Hydraulic Resistance*. CRC Press, 3rd edn. Boca Raton, USA, 790.

Jensen, A., Pedersen, G.K., Wood, D.J. (2003). An experimental study of wave run-up on a steep beach. *J. Fluid Mech.*, 486, 166–188.

Lauber, G. (1997). Experimente zur Talsperrenbruchwelle im glatten geneigten Rechteckkanal. Ph.D. thesis, VAW-ETH, Zürich, Switzerland (in German).

Liem, R., Köngeter, J. (1999). Application of high-speed digital image processing to experiments on dam break waves. *Proc. CADAM Meeting*, Zaragossa, Spain, 399–411.

Mano, A. (1994). Boundary layer developed near surging front. *Coastal Engng. Japan*, 37(1), 23–39.

Peregrine, D.H., Williams, S.M. (2001). Swash overtopping a truncated plane beach. *J. Fluid Mech.*, 440, 391–399.

Ritter, A. (1892). Die Fortpflanzung von Wasserwellen. *Zeitschrift Verein Deutscher Ingenieure*, 36(2), 33, 13 Aug., 947–954 (in German).

Schoklitsch, A. (1917). Über Dambruchwellen. *Kaiserliche Akademie der Wissenschaften, Wien*, Mathematisch-Naturwissenschaftliche Klasse, Sitzungberichte IIa, 126, 1489–1514 (in German).

Wang, Z.Y. (2002). Initiation and mechanism of two phase debris flow. In: Wu *et al.* (eds.), *Proc. Conf. on Flood Defence'2002*, Science Press, New York, 1637–1648.

Whitham, G.B. (1955). The effects of hydraulic resistance in the dam-break problem. *Proc. Roy. Soc. of London, Serie A*, 227, 399–407.